

Constraining the primordial orbits of the Terrestrial Planets

R. Brasser¹, K. J. Walsh² and D. Nesvorný²

¹ *Institute for Astronomy and Astrophysics, Academia Sinica, Taipei 10617, Taiwan*

² *Southwest Research Institute, 1050 Walnut St., Suite 300, Boulder, CO, 80302, USA*

7 July 2018

ABSTRACT

Evidence in the Solar System suggests that the giant planets underwent an epoch of radial migration that was very rapid, with an e-folding timescale shorter than 1 Myr. It is probable that the cause of this migration was that the giant planets experienced an orbital instability that caused them to encounter each other, resulting in radial migration. A promising and heavily studied way to accomplish such a fast migration is for Jupiter to have scattered one of the ice giants outwards; this event has been called the ‘jumping Jupiter’ scenario. Several works suggest that this dynamical instability occurred ‘late’, long after all the planets had formed and the solar nebula had dissipated. Assuming that the terrestrial planets had already formed, then their orbits would have been affected by the migration of the giant planets as many powerful resonances would sweep through the terrestrial planet region. This raises two questions. First, what is the expected increase in dynamical excitement of the terrestrial planet orbits caused by late and very fast giant planet migration? And second, assuming the migration occurred late, can we use this migration of the giant planets to obtain information on the primordial orbits of the terrestrial planets? In this work we attempt to answer both of these questions using numerical simulations. We directly model a large number of terrestrial planet systems and their response to the smooth migration of Jupiter and Saturn, and also two jumping Jupiter simulations. We study the total dynamical excitement of the terrestrial planet system with the Angular Momentum Deficit (AMD) value, including the way it is shared among the planets. We conclude that to reproduce the current AMD with a reasonable probability ($\sim 20\%$) after late rapid giant planet migration and a favourable jumping Jupiter evolution, the primordial AMD should have been lower than $\sim 70\%$ of the current value, but higher than 10%. We find that a late giant planet migration scenario that initially had five giant planets rather than four had a higher probability to satisfy the orbital constraints of the terrestrial planets. Assuming late migration we predict that Mars was initially on an eccentric and inclined orbit while the orbits of Mercury, Venus and Earth were more circular and coplanar. The lower primordial dynamical excitement and the peculiar partitioning between planets impose new constraints for terrestrial planet formation simulations.

Key words: Solar System: general

1 INTRODUCTION

It is thought that the giant planets did not form where they are today but instead have migrated in the past (e.g. Fernandez & Ip, 1984; Hahn & Malhotra, 1999). It is also thought that this migration was not smooth but that instead the outer planets suffered a dynamical instability where at least one ice giant was scattered by Jupiter and Saturn (Thommes et al., 1999). This dynamical instability of the giant planets, and subsequent mutual scattering among them, is the most likely way to explain their current eccentricities and inclinations (Tsiganis et al., 2005; Morbidelli et al., 2009). This episode of mutual scattering ensures that the migration of Jupiter and Saturn was fast enough to keep the asteroid belt stable (Minton & Malhotra, 2009; Morbidelli et al., 2010), and, if this migration occurred late, also the terrestrial planets (Brasser et al.,

2009). A dynamical instability in the outer solar system could also explain many additional features of the outer solar system we observe today: the capture and orbital properties of Jupiter’s Trojans (Morbidelli et al., 2005; Nesvorný et al., 2013), the orbital properties and structure of the Kuiper Belt (Levison et al., 2008), the capture of the irregular satellites of the giant planets (Nesvorný et al., 2007) and, if the migration occurred late, the Late Heavy Bombardment of the terrestrial planets (Gomes et al., 2005; Bottke et al., 2012). Here we assume throughout that the migration of the giant planets coincided with the Late Heavy Bombardment and thus occurred after the formation of the terrestrial planets. We study the consequence of this late dynamical instability of the giant planets on the inner solar system.

Brasser et al. (2009) attempted to reproduce the current

arXiv:1306.0975v1 [astro-ph.EP] 5 Jun 2013

secular architecture of the terrestrial planets in response to late giant planet migration. They showed that the migration of Jupiter and Saturn needed to have been very fast, otherwise the eccentricities of the terrestrial planets would have been excited to values much higher than they are today. The eccentricity excitation is caused by a powerful secular resonance between the terrestrial planets and Jupiter. As Jupiter and Saturn drift apart Jupiter's proper precession frequency, g_5 , decreases and crosses the proper frequencies associated with the terrestrial planets (Brasser et al., 2009; Agnor & Lin, 2012). Thus, the sweeping of g_5 causes the terrestrial planets to experience the secular resonances $g_5 = g_n$, with $n = 1 \dots 4$. Here g_n are the proper eccentricity eigenfrequencies of the terrestrial planets. Both works demonstrated that the crossing of the resonances $g_5 = g_2$ and $g_5 = g_1$ caused the greatest eccentricity increase in Mercury, Venus and Earth because they were crossed slowly. The resonances with g_1 and g_2 occur when the Saturn to Jupiter period ratio is $P_S/P_J \sim 2.25$ and $P_S/P_J \sim 2.15$.

In Brasser et al. (2009) two solutions were presented for solving the problem of keeping the excitation of the orbits of the terrestrial planets at their current level. The first mechanism is one in which the secular resonances $g_5 = g_2$ and $g_5 = g_1$ had a phasing that resulted in the eccentricity either decreasing or that the eccentricity increase in each planet was very small. The probability of this phasing was estimated at approximately 10% (see also Agnor & Lin, 2012). The second mechanism was for the migration of Jupiter and Saturn to have proceeded very quickly by Jupiter scattering one of the ice giants outwards. Energy and angular momentum conservation causes Jupiter to move inwards as it scatters the ice giant outwards and increases the period ratio with Saturn. The typical time scale of Jupiter's migration is 100 kyr. The scattering scenario for Jupiter's migration was dubbed the 'jumping Jupiter' scenario because the semi-major axis of Jupiter appears to undergo a sudden decrease, increasing the period ratio with Saturn. Minton & Malhotra (2009) advocated a short migration time scale based on the structure of the asteroid belt. This led Morbidelli et al. (2010) to expose a model asteroid belt to a jumping Jupiter simulation. They concluded that the migration of the giant planets had to be of this type because it is the only known physical mechanism that can drive such fast migration. This result was further supported by Walsh & Morbidelli (2011), who demonstrated that the migration of Jupiter had to be fast whether this occurred late i.e. at the time of the Late Heavy Bombardment, or right after the gas disc had dissipated. Agnor & Lin (2012) were aware of the difficulty of keeping the terrestrial system stable as the gas giants migrated and for this reason they advocated an early migration, occurring before the terrestrial system had fully formed.

In a separate study Agnor & Lin (2012) investigated the effect of the migration of the giant planets on the terrestrial planets. They kept track of changes in the terrestrial planet's Angular Momentum Deficit (AMD), which is a measure of a system's deviation from being perfectly circular and coplanar (Laskar, 1997). Here we adopted a dimensionless variation, though we shall continue to refer to it as 'AMD' for simplicity. It is defined as (e.g. Raymond et al., 2009)

$$\text{AMD} = \frac{\sum_n m_n \sqrt{a_n} (1 - \sqrt{1 - e_n^2} \cos i_n)}{\sum_n m_n \sqrt{a_n}}, \quad (1)$$

where m is the mass of plane n in units of the Solar mass, a is the semi-major axis of said planet, e is its eccentricity and i is

its inclination with respect to a reference plane (in our case, the invariable plane). Agnor & Lin (2012) noticed that the current distribution of the eccentricity contribution to the AMD is mostly contained in the components corresponding to Mercury and Mars. These two components have a combined total value of 85% of the system's AMD. This led Agnor & Lin (2012) to conclude that late migration of Jupiter and Saturn had to occur with an e-folding time scale $\tau \ll 1$ Myr, otherwise the AMD of the terrestrial planets would be incompatible with its current value. This result is in agreement with Brasser et al. (2009). From their numerical experiments Agnor & Lin (2012) find that the excitation of the eccentricities of the terrestrial planets scales as $\tau^{1/2}$. However, they conclude that when $\tau \lesssim 0.1$ Myr the excitation imposed on the terrestrial planets is independent of τ because the excitation is impulsive rather than adiabatic. In other words, for values of τ shorter than 0.1 Myr the AMD increase of the terrestrial planets is independent of τ and is equal to a constant value. Here we try to determine the magnitude of the excitation of the AMD of the terrestrial planets during this fast migration.

Agnor & Lin (2012) also investigated the most likely primordial orbits of the terrestrial planets that are consistent with this fast late migration. They concluded that the primordial amplitudes of the eccentricity modes associated with Venus and Earth had to be nearly 0. On the other hand the primordial amplitudes of the eccentricity modes corresponding to Mercury and Mars were comparable to their current values. These results suggest that Mercury and Mars were already eccentric (and possibly inclined) before giant planet migration while Earth and Venus obtained their eccentricities after the migration of the gas giants.

In summary, multiple studies point towards a very rapid migration of the giant planets, most likely of the jumping Jupiter variety. If this migration occurred late this raises two questions. First, the terrestrial planets are excited even if the period ratio jumps far enough (beyond 2.3) and the resonances $g_5 = g_1$ and $g_5 = g_2$ are not activated. However, it is not *a priori* clear how much the terrestrial planets are excited if the period ratio jumps beyond 2.3. This raises the issue of what were the initial orbits of terrestrial planets that could meet these constraints. Second, does a jump that does not destabilise the terrestrial planets occur in a statistically significant number of cases? The Jupiter-Saturn period ratio needs to 'jump' from ~ 1.5 to beyond 2.3 and then also avoid moving past the current value of 2.49.

In response to the first question, in this paper we determine how late giant planet migration changed the orbits of the terrestrial planets with the use of numerical simulations. The aim is to provide an upper limit on the primordial AMD of the terrestrial planets. Knowing the possible range of terrestrial planet orbits before the late migration of the giant planets could impose a constraint for models of terrestrial planet accretion. While current terrestrial planet formation simulations are capable of generating systems whose AMD and mass distribution matches the current terrestrials (e.g. Hansen, 2009; Walsh et al., 2011; Raymond et al., 2009), it is possible that late giant planet migration substantially increased the AMD of the terrestrials. Current simulations are unable to form a cold terrestrial system with the right mass distribution. Here we aim to quantify this AMD increase and thus impose a possible new target that terrestrial planet formation simulations should reproduce. We set up mock terrestrial planet systems with different initial AMDs and phasing, and expose them to the instability of

the giant planets. We then statistically analyse the results and determine the resulting orbital structure and AMD values.

Regarding the second question Brassier et al. (2009) concluded that the probability of a jumping Jupiter simulation that kept all four giant planets, and had the period ratio rapidly increase to 2.3 or higher, was very low. This led Nesvorný (2011) to suggest the solar system may have contained a third ice giant that was ejected during the late dynamical instability (see also Batygin et al. 2012). This idea was followed up by Nesvorný & Morbidelli (2012). They ran 10 000 simulations of late giant planet instabilities from a large variety of initial conditions and performed 30 to 100 simulations per set of initial conditions to account for stochastic effects. They included simulations with four, five and six giant planets and imposed four stringent constraints each simulation should fulfil to be considered successful. One of these constraints was that the Jupiter-Saturn period ratio should jump to 2.3 or higher but end below 2.5. The large number of simulations for each set of initial conditions allowed them to quantify the probability of the outcome adhering to all four constraints. With initially four planets the probability was found to be less than 1%, while it increased to 5% for certain configurations of five planets. Thus, it appears that the 5-planet model is a more promising avenue to reproduce the current configuration of the outer planets than a 4-planet case.

The work by Nesvorný & Morbidelli (2012) was just the first simple attempt to trace the dynamical history of the outer planets because the terrestrial planets were not included in their simulations. Instead, they used the simple period ratio constraints from Brassier et al. (2009) and assumed that the terrestrial planets would survive the migration if these were satisfied. Here we include the terrestrial planets in the simulations and expose them to a few cases from the above works to check their behaviour more explicitly.

The aim and methodology of this paper differ from those of Brassier et al. (2009) and Agnor & Lin (2012) in several ways. First, Brassier et al. (2009) only investigated whether the eccentricities of the terrestrial planets could be kept below or at their current values if the gas giants migrated quickly. They did not investigate the range of possible outcomes when the initial phasing of the terrestrials differed at the time of the instability. Agnor & Lin (2012) went further than Brassier et al. (2009) and performed simulations to obtain a more stringent limit on the time scale of the migration of Jupiter and Saturn. However, their simulations were all of the smooth migration variety and were controlled by having a pre-determined finite migration range and time scale. While they measured the probability of keeping the eccentricities of the terrestrial planets below a certain threshold value as a function of the migration e-folding time, they only did so for each planet individually rather than focus on the terrestrials as a system. The approach taken here is to consider the excitation of the whole terrestrial system by measuring the difference between the AMD after and before migration, and the mean value and variance of the final AMD. From there we determine the most likely primordial value of the AMD. We find that if the gas giants' period ratio jumps from 1.5 to beyond 2.3 and remains below 2.5, then the median final AMD of the terrestrial planets equals the current value if they were initially dynamically cold. We also find that Mars had to be more excited than the other three.

This paper is divided as follows. In Section 2 we present the

details of our numerical simulations and their initial conditions. This is followed by the results in Section 3. Section 4 is reserved for the discussion and implications of this work and our conclusions are drawn in the last section.

2 METHODS

The current study is based on a large set of numerical simulations where we subject the terrestrial planets to the effects of the evolution of the migrating giant planets. In principle, we prefer to subject the terrestrial planets to a series of Nice model simulations with fast migration of the giant planets. However, the evolution of the giant planets is chaotic and this makes it difficult to quantify changes in the orbits of the terrestrial planets.

Thus we first performed a series of simulations where we subject the terrestrial planets to smooth migration of the gas giants with various initial values of their period ratio. We set the e-folding time for their smooth migration at $\tau = 3$ Myr and at 1 Myr, where 1 Myr is the shortest time scale we have witnessed to occur in self-consistent smooth migration simulations of the giant planets due to planetesimal scattering; the typical time scale is 3 to 5 Myr (Hahn & Malhotra, 1999; Morbidelli et al., 2010). We also made sure that the final amplitude of the g_5 mode in Jupiter, e_{55} , is close (0.041) to its present value (0.043).

Brassier et al. (2009) and Agnor & Lin (2012) show that during the migration the terrestrial planets experience the effects of the resonances $g_5 = g_2$ at $P_S/P_J \sim 2.15$ and $g_5 = g_1$ at $P_S/P_J \sim 2.25$. Agnor & Lin (2012) further conclude that the current amplitudes of the eccentricity eigenmodes of Mercury and Venus, e_{11} and e_{22} , can only be reproduced when these resonances are crossed on time scales $\tau_2 \lesssim 0.05$ Myr and $\tau_1 \lesssim 0.7$ Myr, respectively. Therefore we ran a large number of smooth migration experiments where we place Jupiter and Saturn on orbits with P_S/P_J ranging from 2.15 to 2.3 in increments of 0.01. The initial conditions mimic a jump to this period ratio. Examples of the evolution of P_S/P_J and the eccentricities of Jupiter and Saturn during these smooth migration simulations are given in Fig. 1.

We quantify the final eccentricities of Mercury and Venus because these two planets are the most vulnerable to the sweeping of g_5 . We consider a simulation outcome to be successful if the maximum eccentricity of Mercury remained below 0.35 and that of Venus below 0.09. These upper limits on the eccentricities of Mercury and Venus are based on the results of Laskar (2008), who showed that long-term chaotic diffusion of the eccentricities and inclinations of the terrestrial planets can significantly alter their mean values from the current ones. Over the age of the solar system Mercury has a 50% chance to have its eccentricity increased above 0.35 when starting at the current value, while Venus has a 50% probability of its eccentricity exceeding 0.09. A second constraint on Mercury's eccentricity comes from its rotation: if its eccentricity had exceeded 0.325 for a long time it would most likely have been trapped in the 2:1 spin-orbit resonance rather than in the current 3:2 (Correia & Laskar, 2010).

The smooth migration simulations were supplemented with Nice-model jumping Jupiter simulations. In this study we show the results of one 4-planet Nice model simulation ('classical Nice') and one 5-planet case (Nesvorný & Morbidelli, 2012). The numer-

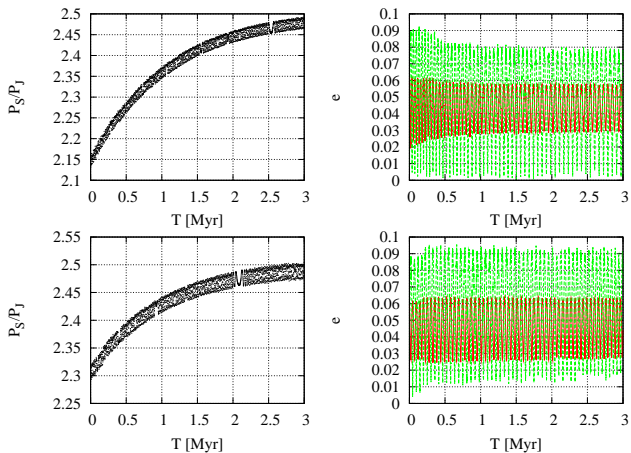


Figure 1. The period ratio P_S/P_J (left panels) and eccentricities of Jupiter (red) and Saturn (green) (right panels) for two of the smooth migration runs. The other simulations have a similar evolution.

ical simulations were performed with SWIFT RMVS3 (Levison & Duncan, 1994), which was modified to read in the evolution of the giant planets and compute their intermediate positions by interpolation (Petit et al., 2001; Brasser et al., 2009; Morbidelli et al., 2010). All the planets from Mercury to Neptune were included in the Nice model simulations, while we included only Mercury to Saturn in the smooth migration runs. We added the effects of general relativity in all our simulations according to the method described in Nobili & Roxburgh (1986). This consisted of adding the effects of a disturbing potential to SWIFT whose effect generates the correct perihelion precession, but does not reproduce the increased orbital frequency (Saha & Tremaine, 1994). This potential is

$$V_{\text{GR}} = -3 \left(\frac{GM_{\odot}}{c} \right)^2 \frac{a}{r^3}, \quad (2)$$

where G is the gravitational constant, M_{\odot} is the Solar mass, c is the speed of light and r is the planet-Sun distance. In all of our simulations the time step was set at 0.02 yr (approximately 7 days). The series of simulations consisted of the following.

First we determined the new initial orbits of the terrestrial planets using the AMD as the independent variable. We chose to base our system on its AMD value and the share in each planet rather than individual orbits because this greatly simplifies the subsequent analysis. We took the current orbits of the terrestrial planets with respect to the Solar System’s invariable plane from the IMCCE’s ephemerides website¹ and computed the instantaneous AMD and the share in each planet. The share of the AMD in each planet is currently 34% in Mercury, 20% in Venus, 21% in Earth and 25% in Mars, and is computed as

$$f_n = \frac{m_n \sqrt{a_n} (1 - \sqrt{1 - e_n^2} \cos i_n)}{\sum_k m_k \sqrt{a_k} (1 - \sqrt{1 - e_k^2} \cos i_k)}. \quad (3)$$

The current AMD value and share in each planet forms our base orbit set. We verified with numerical simulations that the current AMD and the share in each planet are representative of their long-term average values. Second, for each simulation the initial value of the AMD was scaled from the current one. This simple approach allowed us to mimic systems whose primordial AMD

was lower or higher than the current value but with the same partitioning among the planets. For the Nice model simulations we scaled the AMD ranging from 0.1 to 2.2 times the current value in increments of 0.3. The higher values were chosen to determine if destructive interference during giant planet migration could lower the primordial AMD. For the smooth migration experiments this scaling was 0.1, 0.5 and 1.0.

Third, the initial eccentricities and inclinations of the terrestrial planets were calculated by assuming that $e = \sin i$ and by keeping the semi-major axes fixed at their current values. For the smooth migration experiments we also ran a separate set where all the AMD was in Mercury’s eccentricity (so that its initial values were 0.088, 0.195 and 0.276 respectively). The longitude of the ascending node (Ω), argument of pericentre (ω) and mean anomaly (M) of each terrestrial planet were chosen at random on the interval 0 to 360°. This randomisation was done to account for the planets having different phasing when the gas giants migrate.

Fourth, the newly-generated terrestrial systems were subjected to a jumping Jupiter or smooth migration evolution. For the jumping Jupiter cases the final system was integrated with SWIFT RMVS3 for an additional 2 Myr to obtain the averaged final AMD. Last, for the Nice model cases the averaged final AMD value was recorded, together with the *averaged* share of the AMD that each planet possesses. These averages were obtained over the last quarter of the simulations. We also calculated $\langle e \rangle / \langle \sin i \rangle$ for each planet. For the smooth migration experiments we computed the cumulative distributions of Mercury’s and Venus’ minimum, mean and maximum eccentricity and the probability that their maxima are below 0.35 and 0.09 respectively. We ran 300 simulations for each value of the initial AMD to account for statistical effects and phasing. The evolution of the gas giants was kept the same for each simulation. The integrator SWIFT RMVS3 cannot handle close encounters between the planets (Levison & Duncan, 1994) and thus a simulation was stopped when a pair of planets encountered each other’s Hill spheres or when they were farther than 500 AU from the Sun. All simulations were performed on the ASIAA HTCCondor pool.

3 RESULTS

In this section we present the results of our numerical simulations. Rather than discuss all the possible outcomes from each set of simulations, we shall take a more statistical approach.

3.1 Smooth migration experiments

We first studied the effect of smooth migration of Jupiter and Saturn on the terrestrial planets. We focus our attention on Mercury and Venus because these two planets are the most vulnerable to the secular sweeping of g_5 through the terrestrial region. The goal of these simulations is to establish the final eccentricities of Mercury and Venus as a function of initial P_S/P_J and AMD, and the probability that the maximum eccentricity of Mercury remains below 0.35 and that of Venus below 0.09.

¹ <http://www.imcce.fr>

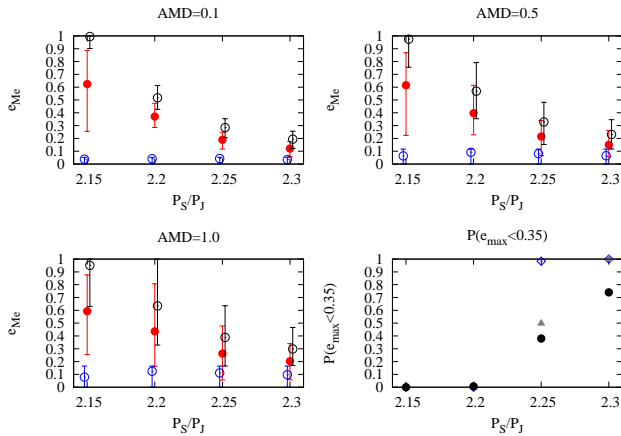


Figure 2. Average minimum eccentricity (blue circles), average mean eccentricity (red bullets) and average maximum eccentricity (black circles) of Mercury as a function of initial Jupiter-Saturn period ratio (top panels and bottom-left panel). The error bars depict the range of eccentricities. Three different initial terrestrial planet AMD values are shown (as a fraction of the current value); 0.1 (upper left), 0.5 (upper right) and 1.0 (lower left). The bottom-right panel depicts the probability for Mercury’s average maximum eccentricity to remain below 0.35 as a function of initial period ratio. The blue diamonds are for low AMD, grey triangles correspond to the run where the AMD was half of the current value case and the bullets are for cases where the AMD equals the current one. For clarity we only depict results in 0.05 increments of initial period ratio.

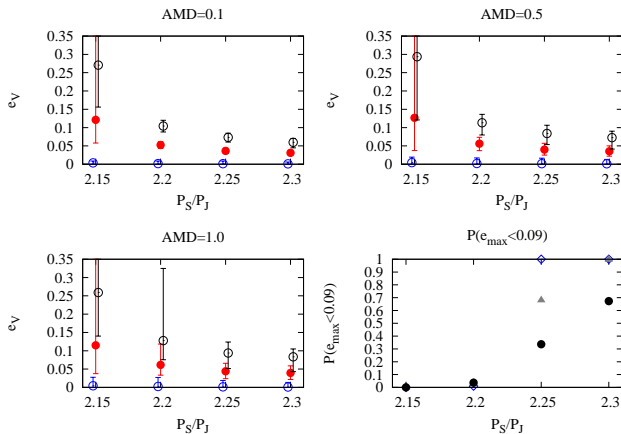


Figure 3. Same as Fig. 2 but here the eccentricity of Venus is plotted. For clarity we only depict results in 0.05 increments of initial period ratio.

3.1.1 Typical migration: $\tau = 3$ Myr

We first simulate Jupiter and Saturn’s migration with an e-folding time scale of $\tau = 3$ Myr, which is a typical value found in smooth migration simulations (Hahn & Malhotra, 1999). We kept the amplitude of Jupiter’s eccentricity eigenmode term, e_{55} , as close as possible to its current value to best mimic the effect of the sweeping of the g_5 frequency. We placed Jupiter and Saturn on orbits with initial period ratio between 2.15 and 2.3 in increments of 0.01. The AMD of the terrestrial planets was then scaled to either a tenth (0.1), half (0.5) or equal to the current value. The AMD was either shared among the planets as is found today, or put entirely into the orbit of Mercury. We have presented the results in a series of four figures.

Figure 2 plots the averages of the minimum eccentricity (blue), the mean eccentricity (red) and the maximum eccentricity (black) of Mercury as a function of initial P_S/P_J for several initial terrestrial planet AMD. The initial AMD sharing among each planet was kept at the current one. The error bars depict the variation of each quantity, and the averages were computed from data taken during the last 0.5 Myr of the migration simulations. The data points for the average minimum and maximum eccentricity have a slight horizontal offset from the mean for clarity. There are two visible trends.

First, the final eccentricity of Mercury decreased as the initial P_S/P_J was increased from 2.15 to 2.3. When the initial period ratio is at 2.15, both the $g_5 = g_2$ and $g_5 = g_1$ resonances are crossed, but when the initial period ratio is beyond 2.2, only $g_5 = g_1$ is crossed. The second trend is that the mean values and the spread increase with initial AMD (comparing the upper left with the upper right and the lower left panels of the two figures). The spread in the average mean and average maximum values decrease slightly with P_S/P_J .

The bottom-right panel of Fig. 2 depicts the probability that the maximum eccentricity of Mercury stays below 0.35. The blue squares correspond to the case with low initial AMD (0.1), the grey triangles are for half AMD (0.5) and the bullets correspond to the cases with current AMD (1.0). The probability increases with increasing period ratio, and reaches near unity for the low-AMD case (0.1) when the initial period ratio is higher than 2.25. Larger values of initial AMD require a period ratio of 2.3 or above. When the initial period ratio is lower than 2.2 the chance of keeping Mercury’s eccentricity in check is zero.

The same procedure is repeated for Venus in Fig. 3. We restricted the calculation to the probability of Venus’ maximum eccentricity staying below 0.09 rather than repeating Agnor & Lin (2012) and requiring that the amplitude of Venus’ eccentricity eigenmode $e_{22} < 0.02$. The probability of acceptable eccentricity for Venus as a function of P_S/P_J is very similar to that found for Mercury (a comparison of the lower right panels of Figures 2 and 3). Probabilities for all cases were $\sim 0\%$ for $P_S/P_J < 2.2$, and $\gtrsim 80\%$ for $P_S/P_J > 2.3$ for both planets; extrapolation suggests that all probabilities reach unity when the period ratio exceeds 2.35.

In summary, we have demonstrated that the smooth migration of Jupiter and Saturn with $\tau = 3$ Myr is only capable of reproducing the current eccentricities of Mercury and Venus with a high probability from a period ratio of 2.25 or higher if the original AMD was very low; otherwise the period ratio should exceed 2.3. However, we did not investigate the effect of changing the migration time scale. This is done below.

3.1.2 Fast migration: $\tau = 1$ Myr

Above we investigated how the terrestrial planets respond to smooth migration of Jupiter and Saturn starting from $P_S/P_J = 2.15$ to 2.30 and migrating to their current period ratio. We concluded that the eccentricities of Mercury and Venus are compatible with their current values when the jump proceeds to 2.3 or beyond. However, we only focused on the typical migration time scale of $\tau = 3$ Myr. Agnor & Lin (2012) demonstrated that the increase in the eccentricities of the terrestrial planets scales as

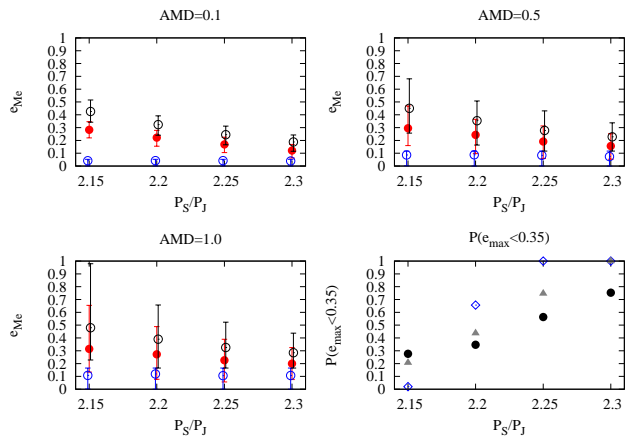


Figure 4. The same as Fig. 2 but now $\tau = 1$ Myr.

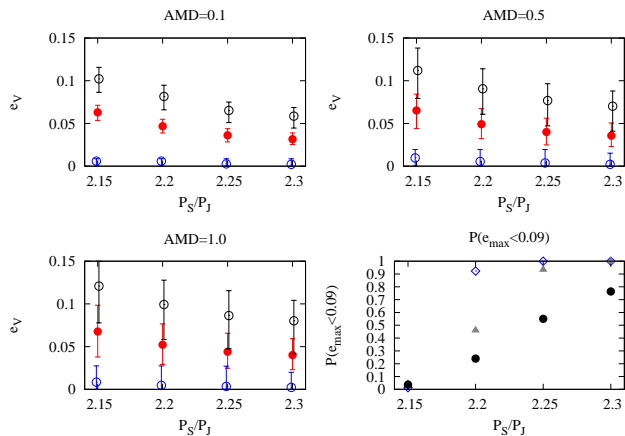


Figure 5. The same as Fig. 3 but now $\tau = 1$ Myr.

$\tau^{1/2}$. However, it is not known how the spread in the eccentricity, and thus the probability of keeping it below a specified value, scales with τ . Therefore, we have performed smooth migration experiments where $\tau = 1$ Myr, which is the lowest value found to occur in Nice model simulations after the period ratio jump. This migration speed is considered to be an extreme case.

The results are plotted in Figs. 4 and 5, and are similar to that found for $\tau = 3$ Myr. The primary difference is that there is a non-zero probability for acceptable eccentricities of Venus and Mercury for period ratios below 2.2, whereas this was essentially zero for the longer time scale migration. However, the spread in the final eccentricity does not seem to strongly depend on τ .

In these smooth migration experiments we tested two different migration time scales. They both produce largely similar results, which are summarised in Table 1. The eccentricities of both Mercury and Venus can be reproduced with a high probability when i) the period ratio P_S/P_J jumps directly to 2.3, ii) the period ratio P_S/P_J jumps to 2.25 if the AMD was initially ~ 0.5 of today's value or iii) the period ratio P_S/P_J jumps to 2.2, the AMD was low and the migration was then very fast ($\tau \sim 1$ Myr).

The above smooth migration tests were designed to mimic the evolution after a ‘jump’, but by starting the simulation at a given

P_S/P_J	Initial AMD			Initial AMD		
	0.1	0.5	1.0	0.1	0.5	1.0
	$\tau = 1$ Myr			$\tau = 3$ Myr		
2.15	✗	✗	✗	✗	✗	✗
2.20	✓	✗	✗	✗	✗	✗
2.25	✓	✓	✓	✓	✓	✗
2.30	✓	✓	✓	✓	✓	✓

Table 1. A summary of the Figures 2-5, where a set of parameters received a ✓ if both Mercury and Venus had acceptable maximum eccentricities ($e < 0.35$ and $e < 0.09$ respectively) in at least 50% of the simulations tested at that set of parameters. Otherwise we placed a ✗.

period ratio P_S/P_J they did not explicitly model the actual jump. Therefore these results are likely optimistic for maintaining an acceptable system AMD for any given simulation. We now turn our focus on subjecting the terrestrial system to some Nice model simulations, in order to quantify how the system of terrestrial planets responds to the actual ‘jump’ of period ratio P_S/P_J . We discuss the results of these experiments in the next subsections.

3.2 A 4-planet Nice model simulation

In the previous subsection we have demonstrated that it may be possible to reproduce the current eccentricities of Mercury and Venus after the giant planets underwent a late instability, provided that some criteria are met about the evolution of the gas giants. The reproduction becomes more likely when the orbits of the terrestrials were dynamically colder than today. Here we demonstrate a case of a 4-planet Nice model simulation that meets these criteria but that nevertheless fails to reproduce the current terrestrial system due to a surprising resonant interaction with an ice giant.

The first 10 Myr of the evolution of the giant planets in the test 4-planet Nice model simulation is displayed in Fig. 6. The simulation was run for 100 Myr but after 10 Myr the gas giants had settled on their final orbits and the migrating ice giants have little effect on the terrestrials. At the end of the migration Uranus and Neptune are closer to Jupiter and Saturn than they are today, which increases the precession frequencies of all the giant planets. The period ratio of the gas giants jumps to about 2.23 and then increases to beyond 2.4 within 4 Myr, so that $\tau \sim 1$ -1.3 Myr. Thus, the simulation appears to be compatible with the conditions we imposed from the smooth migration experiments: i) a jump to approximately 2.25 or higher, and ii) subsequent smooth migration on a time scale of $\tau \sim 1$ Myr. This simulation satisfies almost all conditions imposed by Nesvorný (2011) and Nesvorný & Morbidelli (2012): only the final semi-major axis of Uranus is too low and its inclination is too high. Their other criteria – having four planets at the end, having the amplitude of the Jovian eccentricity eigenmode $e_{55} > 0.022$, having P_S/P_J jump from < 2.1 to > 2.3 in a time span shorter than 1 Myr – are all matched. The final semi-major axes are 5.15, 9.32, 15.2 and 24.5, eccentricities are 0.027, 0.073, 0.042 and 0.009, inclinations with respect to the invariable plane are 0.54° , 1.78° , 2.43° and 0.55° , and $e_{55} = 0.0342$, close to 80% of the current value. The amplitude of the latter bears direct correlation to the dynamical excitation of the terrestrial planets (Brasser et al., 2009; Agnor & Lin, 2012)..

In Fig. 7 we plot the cumulative distribution of the AMD of

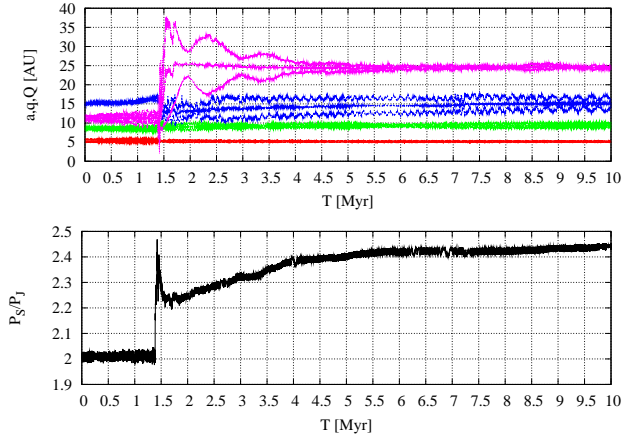


Figure 6. Evolution of the semi-major axis, perihelion and aphelion of the giant planets (top panel) and the Jupiter-Saturn period ratio (bottom panel) for the jumping Jupiter simulation used here. Red is Jupiter, green is Saturn, blue is Uranus and magenta is Neptune.

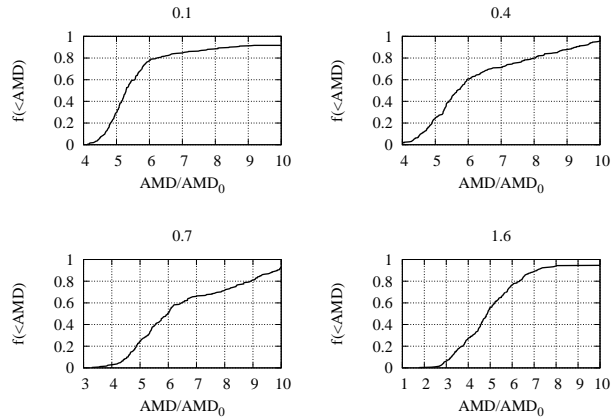


Figure 7. Cumulative distributions of the AMD of the terrestrial planets after the migration of the giant planets for various initial AMD values. The evolution of the giant planets is displayed in Fig. 6.

the terrestrial planets after the migration of the giant planets for various initial values of the AMD. The headers above each panel depict the initial fraction of the current AMD. There are several interesting features. First, even when the terrestrials are originally very cold ($AMD = 0.1$), the minimum AMD after migration is more than 3 times the current value, with a median value near 4. Increasing the initial AMD also increases the final median value. Second, the AMD almost always increases, and thus the probability of destructive interference – which causes an overall reduction in the AMD – is much lower than the $\sim 10\%$ found by Brasser et al. (2009) and Agnor & Lin (2012). In order to understand why the AMD increases by such a large amount, we plot an example of the evolution of the terrestrials below.

Figure 8 shows the evolution of the eccentricity and inclination of the terrestrial planets (top and top-middle panels). The colour coding is grey for Mercury, yellow for Venus, blue for Earth and red for Mars. In the bottom-middle panel we plot the angles $\Delta\varpi_{Me-J} = \varpi_{Me} - \varpi_J$ in black and $\Delta\varpi_{V-J} = \varpi_V - \varpi_J$ in yellow. The bottom panel shows the evolution of P_S/P_J . Immediately after the instability the argument $\Delta\varpi_{Me-J}$ librates with a

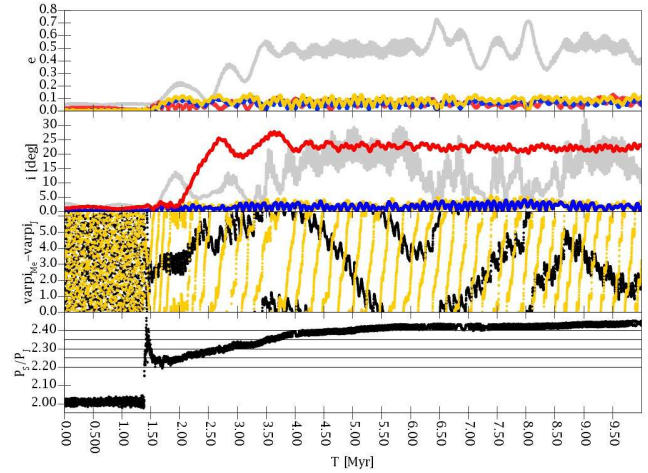


Figure 8. Evolution of the eccentricities (top), inclinations (second-from-top), $\varpi_{Me} - \varpi_J$ (grey) and $\varpi_V - \varpi_J$ (yellow) (third-from-top) and P_S/P_J (bottom panel). The colour coding is grey for Mercury, yellow for Venus, blue for Earth and red for Mars.

long period. This secular resonance between Jupiter and Mercury substantially increases Mercury’s eccentricity before it settles near 0.6. The increase in Mercury’s inclination from roughly 1° to approximately 10° is caused by a secular resonance with Venus: the argument $\Omega_{Me} - \Omega_V$ changes the direction of circulation. The later increase at $t = 8$ Myr is also caused by interaction with Venus.

The second feature is the sudden increase in Mars’ inclination at $t = 1.5$ Myr. This increase is caused by a secular resonance with Uranus (not shown): the argument $\Omega_{Ma} - \Omega_U$ slows down, librates around 0° for one oscillation with period 1 Myr and then continues to circulate. During this libration Mars experiences its rapid increase in its inclination. The temporary coupling between Uranus and Mars demonstrates that the evolution of the ice giants could play an important role in shaping the secular architecture of the inner planets: during the migration phase, when the eccentricities and inclinations of the ice giants are much higher than they are now, they may interact with the terrestrial planets directly. It also demonstrates the importance of the ice giants obtaining their current orbits at the end of the migration phase, which this simulation does not adequately do.

One aspect that merits discussion is how our results depend on the amplitude of the Jovian eccentricity eigenmode e_{55} . Jupiter’s eccentricity forcing is present in the eccentricities of all the terrestrial planets (e.g. Brouwer & van Woerkom, 1950). The amplitude of Jupiter’s forcing term on the terrestrials is directly proportional to e_{55} itself. In this simulation the final amplitude is lower than the current one, so that we would expect the final terrestrial AMD to be lower than its current value. Yet the strange behaviour of Mercury and Mars during the migration substantially increases the final AMD of the terrestrial system. A lower amplitude of the Jovian e_{55} mode could have decreased the final AMD but it would be inconsistent with the current secular architecture of the Solar System and not be sufficient to compensate for the increased AMD values of Mercury and Mars. In conclusion, the evolution of the giant planets needs to excite e_{55} to a value comparable to the current one without any of the terrestrial planets getting caught in a secular resonance.

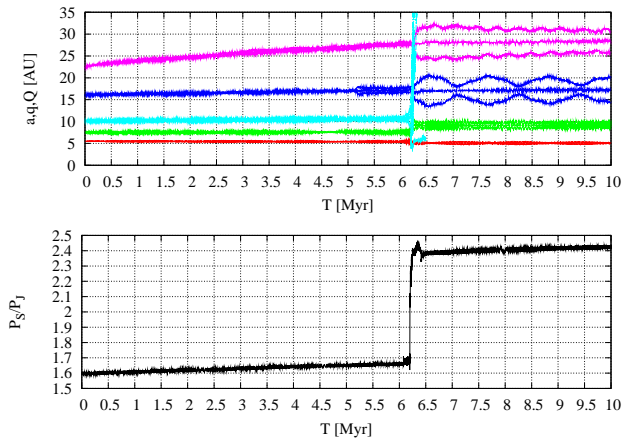


Figure 9. Evolution of the semi-major axes, perihelia and aphelia of a 5-planet Nice model simulation (top panel) and the Jupiter-Saturn period ratio (bottom panel). Red is Jupiter, green is Saturn, blue is Uranus and magenta is Neptune. The colour for the 5th planet is cyan.

As mentioned previously this particular simulation satisfies all of the constraints laid out in the models of Nesvorný (2011) and Nesvorný & Morbidelli (2012) for giant planet migration. Therefore it may be considered as a best case scenario for a jumping Jupiter evolution of the giant planets in regards to their influence on the terrestrial planets.

This simulation demonstrates that Mercury and Mars are more susceptible than Venus and Earth to the evolution of the outer planets. Of course the Earth (and Venus) also suffer the same secular resonance with Uranus that Mars does because $s_3 \sim s_4$, but because of its larger inertia the Earth’s share of the AMD increases a lower amount than Mars’.

From the above results it appears that the migration of the giant planets should proceed on an even shorter time scale, with little to no migration of Jupiter and Saturn occurring after the jump and keeping the e_{55} mode at a value lower than or equal to the current one. Similarly, a jump only to 2.25 may have aggravated this particular case, and a jump to 2.3 may be essential – as was demonstrated in the previous section. Nesvorný & Morbidelli (2012) show that this is very unlikely for a 4-planet case (with probability lower than 1%). However, we found one such case with initially 5 planets in the simulations of Nesvorný & Morbidelli (2012). Thus in the next subsection we present the outcome of a 5-planet Nice model run that matches our criteria.

3.3 A 5-planet Nice model simulation

In this subsection we report on the results of exposing the terrestrial system to a 5-planet Nice model simulation, which was taken from Nesvorný & Morbidelli (2012). The planets started in a quintuple resonant configuration: 3:2,3:2,2:1,3:2. The extra ice giant’s mass was equal to that of Neptune and the planetesimal disc mass was $20 M_{\oplus}$. The evolution of the system for the first 10 Myr is displayed in Fig. 9. The innermost ice giant (cyan) is ejected after 6.3 Myr, right after it is first scattered inwards by Saturn and then immediately ejected by Jupiter, resulting in the big jump in P_S/P_J . There is very little subsequent migration of the gas giants because the mass of the planetesimal disc outside of Neptune was much lower than in the 4-planet case (Nesvorný &

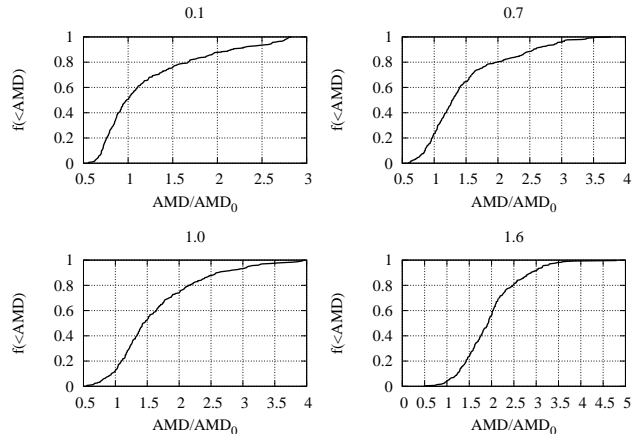


Figure 10. Same as Fig. 7 but now after the 5-planet Nice model simulation.

Morbidelli, 2012). At this stage both Uranus and Neptune end up too close to the Sun, although they are farther than in the 4-planet case. This simulation satisfies almost all conditions imposed by Nesvorný (2011) and Nesvorný & Morbidelli (2012): only the final eccentricity of Uranus is too high. Their other criteria are all satisfied. The final semi-major axes are 5.06, 9.16, 17.2 and 28.2, eccentricities are 0.015, 0.061, 0.171 and 0.082, inclinations with respect to the invariable plane are 0.58° , 1.50° , 1.08° and 0.63° , and $e_{55} \sim 0.04$, close to the current value. We want to stress that we have only used the first 10 Myr of this simulation because later stages only featured slow migration and damping of Uranus and Neptune which is unlikely to strongly affect the terrestrial planets. At the end of the simulation, all criteria from Nesvorný (2011) and Nesvorný & Morbidelli (2012) are satisfied.

In our simulations we compute the inclinations of all planets with respect to the invariable plane at the beginning of the simulation. The mutual scattering of the giant planets and the ejection of an ice giant changes the total angular momentum vector and thus the invariable plane. We checked the simulations for a sudden jump in the inclinations of the terrestrial planets when the first ice giant was ejected but witnessed no such behaviour. In addition, dynamical friction from the planetesimals in the original simulations damped the inclinations of the giant planets, which also changes the invariable plane. Thus, for simplicity, we pinned the inclinations to the invariable plane at the beginning of the simulation.

The AMD response of the terrestrial system to the evolution of the giant planets is depicted in Fig. 10. This figure should be compared to Fig. 7 for the 4-planet case. One may see that the AMD excitation in this simulation is much lower than for the 4-planet case. The top-left panel shows that for a low AMD (0.1) the median final AMD equals the current value. Even when the initial AMD was equal to the current value, it is still reproduced 10% of the time. Though the smooth migration simulations suggested that the primordial AMD of the terrestrial planets had to be very low, the outcome of the 5-planet case shows that the current AMD can be reproduced with a reasonable probability if the primordial value was as high as 70% of the current one (reproduced $\sim 20\%$ of the time). The results from this simulation also demonstrate that destructive interference occurs at most with a $\sim 10\%$ probability (Brasser et al., 2009; Agnor & Lin, 2012), but is not strong enough

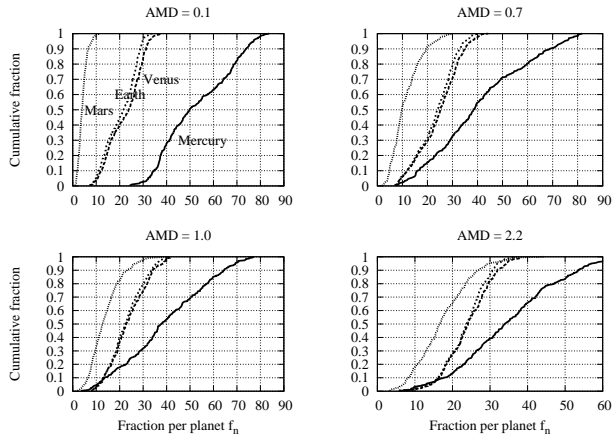


Figure 11. Cumulative distributions of the fraction of the total AMD in each terrestrial planet, f_n – see equation (3). The headers above the panels indicate the amount of original AMD.

to reduce an initially higher AMD (> 1.0) to the current system (AMD ~ 1.0) with a reasonable ($>10\%$) probability (see the bottom right panel of Fig. 10 for an example of an initial AMD of 1.6).

How is the AMD shared among the terrestrial planets after the migration of the giant planets: does the share in each planet stay roughly the same, or are they substantially altered? After each simulation we record the average final AMD and the average share or fraction of the total in each planet, f_n – see equation (3). We plot the cumulative distribution of f_n for various initial AMD values in Fig. 11. This figure serves to illustrate the spread of the share in each planet and thus the amount of excitation relative to the other planets. The value of the primordial AMD are shown above the panel. The fraction of the AMD in Venus or Earth is very similar due to their strong coupling: for all simulations the share of the AMD in both Venus and Earth ranges from 10% to about 40%. The share in Mars increases with increasing AMD, and it typically has between 0 to 20%. The spread in Mercury is much larger than that of the other planets, though it does decrease slightly with increasing AMD. In half of all simulations 50% of the AMD of the terrestrial system is taken up by Mercury, so that the other three planets combined also have 50% and are thus dynamically colder. Most likely at higher AMD some of the excess from Mercury is transferred to Mars. However, for all intents and purposes the final share in each planet appears independent of the original AMD value. For the cold initial system (AMD=0.1) Mars’ value is systematically much lower than found today and Mercury’s is mostly higher. This suggests that Mars experiences little change in its orbit and loses AMD to the other planets because the other three planets gain AMD. Mercury, especially, must have been forced by some mechanism. For higher initial AMD all planets can exchange AMD with each other and the relative forcing of the inner three during the instability compared to Mars is smaller, hence Mars’ share appears to increase with increasing AMD.

When examining the evolution of the giant planets and comparing it with the terrestrial planets we find that Mercury gets caught in the resonance $g_7 = g_1$: after the innermost ice giant is ejected $g_7 \sim 5.3$ "/yr, which is close to g_1 (5.5 "/yr). For reference, currently $g_7 \sim 3.1$ "/yr. To examine the severity of this secular resonance we plot in Fig. 12 the averaged minimum, mean and maximum eccentricities of Mercury (top-left) and Venus

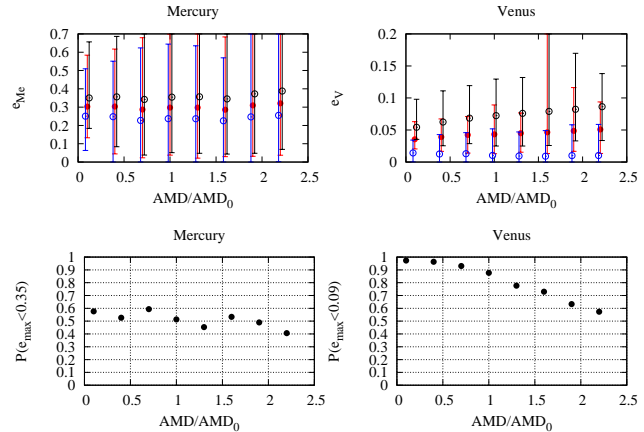


Figure 12. Averaged minimum, mean and maximum eccentricity for Mercury (top-right) and Venus (top-left) as a function of initial AMD. The bottom panels depict the probability of Mercury’s eccentricity staying below 0.35 (left) and Venus’ below 0.09 (right).

(top-right) as a function of the initial AMD. Also plotted is the probability of their maximum eccentricities remaining below 0.35 and 0.09 respectively (bottom-left for Mercury and bottom-right for Venus). For low to mid-AMD values Venus remains low but for all AMD values Mercury’s mean eccentricity is ~ 0.3 and the probability of it being below 0.35 is just over 50%. This is acceptable given that Uranus’ final position is too close to the Sun. Subsequent chaotic diffusion may lower Mercury’s eccentricity to its current value (Laskar, 2008).

Was there any way to avoid Mercury’s high eccentricity? We have stated earlier that we have only used the first 10 Myr of the simulation. Having run for longer would not have solved the issue of Mercury’s high eccentricity because the secular resonance crossing with Uranus would still have occurred on a similar time scale (~ 10 Myr) and yielded a similar increase in Mercury’s eccentricity.

It appears that the giant planet evolution presented in Fig. 9 is mostly capable of reproducing the current AMD of the terrestrial planets with a reasonable probability ($\sim 20\%$), provided the initial AMD remained below 70% of the current value. If the AMD had been equal to the current value the probability for it to remain unchanged is approximately 10%. The lowest initial AMD value reproduced the current AMD of the terrestrial planets in 50% of the simulations. The simulation has more difficulty in reproducing the current fractions of AMD in each planet. However, Mercury’s high eccentricity in these simulations is an artefact of Uranus ending up too close to the Sun. Mars is more difficult. The inner three planets are forced more during the instability than Mars itself, so that the gain of AMD of the inner three occurs at the expense of Mars. Its final low share of the system AMD could be increased to its current value if its original share had been higher than the other three planets i.e. if we had used a different sharing among the planets at the beginning of our simulations. The question then becomes how high this initial share can be pushed and whether we consider a final share of $<10\%$ to be a successful outcome. In the next section, we compare the outcome of our simulations with those of terrestrial planet formation simulations and discuss its implications.

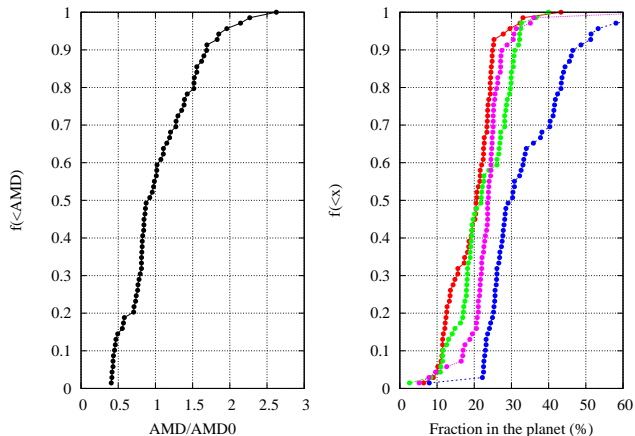


Figure 13. Cumulative value of the final AMD of the 4-planet terrestrial planets systems of Walsh et al. (2011) (right panel). The curve is taken from combining the results of several simulations. The left panel shows the cumulative distribution of the share of the AMD in each planet. Red bullets are the innermost planet, blue and green are for the middle two planets and the magenta corresponds to the outermost planet.

4 COMPARISON WITH TERRESTRIAL PLANET FORMATION SIMULATIONS AND IMPLICATIONS

We have set up a high number of fictitious terrestrial systems and exposed them to the evolution of the migrating giant planets. We have assumed that this migration of the giant planets occurred late and the terrestrial planets had already formed. Some of our results require further explanation, which we do here. We also compare our results with the outcome of terrestrial planet formation simulations.

First, assuming late migration we suggest that the primordial AMD of the terrestrial planets was not only lower than its current value but also that most, or all, of it was contained in Mars. Agnor & Lin (2012), while not investigating the change in AMD directly, also concluded that the primordial orbit of Mars (and Mercury) had to be more excited than those of Venus and Earth. Is this outcome, and the lower AMD that we advocate here, consistent with terrestrial planet formation simulations? To date the simulations best reproducing the current mass–semi-major axis distribution of the terrestrial planets are those of Hansen (2009) and Walsh et al. (2011). Hansen (2009) ran numerical simulations of the formation of the terrestrial planets by placing 400 equal-mass embryos in an annulus from 0.7 AU to 1 AU. The total mass of the embryos was $2 M_{\oplus}$. Walsh et al. (2011) used the migration of Jupiter and Saturn to reproduce the outer edge of the planetesimal disc and recreate the initial conditions of Hansen (2009). Unlike Hansen (2009) Walsh et al. (2011) included planetesimals in their simulations.

We took the data from Walsh et al. (2011) and only kept the cases with four terrestrial planets. We simulated these systems for 1 Myr with SWIFT MVS (Levison & Duncan, 1994) to obtain their averaged AMD, the share of the AMD in each planet and the partitioning of the AMD among eccentricity and inclination. The results are displayed in Fig. 13. The cumulative AMD, normalised to the current value, is displayed in the left panel, where the plot was generated by combining the results of several simulations. In the right panel the share of the AMD in each planet is depicted. The red dots correspond to the innermost planet, followed by green and blue while the magenta dots pertain to the outermost planet.

It appears that the share of the AMD in each planet typically ranges from 10% to 40%, with a median around 25%. This strongly suggests that during the formation process the system reaches angular momentum equipartition. For the current solar system these fractions are 34% in Mercury, 20% in Venus, 21% in Earth and 25% in Mars. Thus the current partitioning among the terrestrial planets in the current solar system is consistent with their primordial ones, though it could be argued that Mercury’s share reflects some additional excitation.

However, the primordial AMD sharing that would most likely lead to the current system (a higher share in Mars than in the other planets), does not closely match the results of Walsh et al. (2011) (Fig. 13). The lowest system AMD from the Walsh et al. (2011) simulations (Fig. 13 left panel) is approximately 40% of the current one. Such a low primordial AMD has been shown in this work to have a high probability of not exceeding the current value following late giant planet migration.

The higher share of Mars is of more concern. In the previous section we demonstrated that cases with a very low AMD yield a share in Mars that is inconsistent with the results presented in Fig. 13, and thus we are inclined to reject a very low primordial AMD of the terrestrial planets. However, Walsh et al. (2011) included planetesimals in their simulations, and these damp the eccentricities of the terrestrial planets through dynamical friction (e.g. O’Brien et al., 2006). Therefore the formation of a lower-AMD system with a nearly-circular and nearly-coplanar Mercury, Venus and Earth and slightly eccentric and inclined Mars cannot be ruled out if the original mass in planetesimals was higher than that in embryos and more confined to a narrower region inside of Mars. It is likely that Mars is a stranded planetary embryo (e.g. Dauphas & Pourmand, 2011) and both Mercury and Mars probably ended up at their current positions by encounters with Venus and Earth (Hansen, 2009; Walsh et al., 2011). These encounters increased their eccentricities and inclinations, and their subsequent isolation from other planetary embryos explains both their small size and continued excited orbits. The lower density of small bodies at these planets’ orbits would have decreased the amount of dynamical friction they experienced and thus their orbits remained hotter than those of Venus and Earth and their AMD share could have also remained higher. New terrestrial planet formation simulations need to explore whether such an outcome is possible.

Second, one could ask the question whether we could have done anything differently. Are the Nice model simulations that we used representative of what happened at that time? Nesvorný (2011) and Nesvorný & Morbidelli (2012) developed a set of criteria of what they deemed a successful Nice model simulation. As stated earlier, they used both four and five giant planets. They reported that to fulfil all of their criteria with a four-planet case the probability is lower than 1%, while in the five-planet case the probability is at most 5%. Thus, in choosing our simulations we decided to opt for the one that gave the best possible jump of Jupiter, while relaxing the criterion of all planets ending at their current semi-major axes. Our choice of simulations are a best case in which the AMD excitation of the terrestrials may be minimised. We justify this choice by repeating that our goal was to try to determine whether the current excitation could be reproduced by late planet migration. To that end the 5-planet case appears to have succeeded.

At minimum the period ratio P_S/P_J needs to jump from < 2.1 to > 2.3 but still stay below 2.5. This constraint holds both for early (Walsh & Morbidelli, 2011) and late migration (Brasser et al., 2009; Agnor & Lin, 2012). It is likely that the primordial period ratio was $P_S/P_J \sim 1.5$ (Morbidelli et al., 2007; Pierens & Nelson, 2008), and thus the jump may have needed to proceed from a period ratio of ~ 1.5 to > 2.3 . This jump occurred in the 5-planet simulation presented here but it is substantial and difficult to accomplish by encounters with an ice giant, even when the latter is ejected (Nesvorný & Morbidelli, 2012).

Unfortunately, during late migration the terrestrial planets are not entirely unaffected by the ice giants' evolution. Despite the ice giants' influence we argue that the final outcome may not change substantially when the ice giants undergo a different evolution: the largest threat to the stability of the terrestrial planets is the sweeping of g_5 through the terrestrial region. Therefore, any simulation keeping (all) four planets may be satisfactory, provided that the period ratio P_S/P_J undergoes the required jump to 2.3 in a short enough time scale ($\tau \sim 0.1$ Myr) and suffers little migration afterwards (Nesvorný & Morbidelli, 2012).

Another issue that warrants a discussion are the initial conditions of the terrestrial planets. For the sake of simplicity we have taken the system AMD to be the independent variable rather than the eccentricity and inclination of each planet. We randomised the phases and ran a large number of simulations to determine a range of outcomes. We performed a statistical analysis rather than a case-by-case investigation. However, we also decided to partition the z -component of the angular momentum $h_z = \sqrt{1-e^2} \cos i$ evenly among inclination and eccentricity, inspired by the results of the simulations by Hansen (2009) and Walsh et al. (2011). Would the results have changed substantially if we had done this differently e.g. by setting $e = \frac{3}{2} \sin i$? The AMD partitioning is altered by the migration of the giant planets and thus the final sharing of the AMD can be changed by applying a different primordial distribution among the planets. Thus we think that our choice of setting $e = \sin i$ is justified.

The last issue pertains to the sharing of the AMD among the terrestrial planets. In our simulations we decided to keep each planet's current share but we could have made this a random variable as well, limiting it to the range displayed in the right panel of Figs. 13. Once again we opted for simplicity in using the current values. For low initial AMD the shares of Mercury, Venus and Earth show a reasonable dispersion at the end of the 5-planet simulation. The only planet whose share remains low is Mars, but we can use the argument above that it was originally hotter than the other planets to offset its final low AMD. The conclusion of Mars being originally dynamically hotter was also reached by Agnor & Lin (2012). Changing the original sharing will add an extra layer of complexity to the problem that becomes somewhat speculative and it may no longer be possible to make any predictions about the original AMD. Thus we decided to use the current partitioning. However, Mars' low final share does suggest that very low primordial AMD values may not be consistent with excitation of the AMD by late giant planet migration.

5 CONCLUSION

In this study we investigated in detail how the orbits of the terrestrial planets change when the giant planets undergo their late instability. Based on criteria developed in Brasser et al. (2009), Agnor & Lin (2012) and Nesvorný & Morbidelli (2012) we subjected the terrestrial planets to two jumping Jupiter Nice model simulations. Thus the migration of Jupiter and Saturn occurs on a time scale $\tau < 0.1$ Myr and were best-case scenarios for both a 4-planet and 5-planet evolution, in which the duration of the jump of Jupiter was the shortest. We chose the initial AMD of the terrestrial planets as the independent variable and ran many simulations with random phasing of the orbital angles of the terrestrial planets. We recorded the final AMD of the terrestrial system and the sharing of the AMD among the terrestrial planets.

From the numerical simulations that we performed three basic conclusions are drawn. First, if the late giant planet migration scenario that we subjected the terrestrial planets to are representative of the reality, and to reproduce the current AMD with a reasonable probability ($\sim 20\%$), the primordial AMD of the terrestrial planets should have been lower than 70% of the current value. If the primordial AMD had been higher than the current value, the probability of the terrestrial planets ending up with their current AMD value becomes very low ($< 1\%$). However, a very low primordial AMD (~ 0.1) can probably be ruled out because the final share in Mars is inconsistent with the results of Walsh et al. (2011).

Second, at present the terrestrial planets carry approximately equal amounts of the system's AMD. Assuming that their orbits were influenced by late giant planet migration the primordial partitioning among the planets must have been peculiar because the evolution of the giant planets left Mars' orbit mostly intact; hence most (or perhaps all) of the primordial AMD was taken up by Mars because after migration it lost most of its share to the other planets. From this configuration and the initially low AMD (0.4-0.7) we predict that Mars' primordial eccentricity and inclination were similar to their current values. Mercury, Venus and Earth were approximately circular and coplanar. The low primordial AMD and the peculiar partitioning impose a new constraint for terrestrial planet formation simulations.

Third, the Jupiter-Saturn period ratio had to have jumped from ~ 1.5 to beyond 2.3 with little subsequent migration. Having little subsequent migration is needed to keep the final terrestrial planet AMD at the current value when starting from a lower one. This evolution of the giant planets is better realised with 5 planets than with 4 (Nesvorný & Morbidelli, 2012).

6 ACKNOWLEDGEMENTS

The Condor Software Program (HTCondor) was developed by the Condor Team at the Computer Sciences Department of the University of Wisconsin-Madison. All rights, title, and interest in HTCondor are owned by the Condor Team. Support for KJW came from the Center for Lunar Origin and Evolution of NASA's Lunar Science Institute at the Southwest Research Institute in Boulder, CO, USA. We thank an anonymous reviewer for valuable feedback that improved this manuscript.

7 REFERENCES

- Agnor C. B., Lin D. N. C., 2012, *ApJ*, 745, 143
- Batygin K., Brown M. E., Betts H., 2012, *ApJ*, 744, L3
- Bottke W. F., Vokrouhlický D., Minton D., Nesvorný D., Morbidelli A., Brasser R., Simonson B., Levison H. F., 2012, *Natur*, 485, 78
- Brouwer, D., van Woerkom, A. J. J. 1950. *Astron. Papers Amer. Ephem.* 13, 81-107.
- Brasser R., Morbidelli A., Gomes R., Tsiganis K., Levison H. F., 2009, *A&A*, 507, 1053
- Correia A. C. M., Laskar J., 2010, *Icar*, 205, 338
- Dauphas N., Pourmand A., 2011, *Nature*, 473, 489
- Fernandez, J.A., Ip, W.-H., 1984, *Icarus* 58 109
- Gomes R., Levison H. F., Tsiganis K., Morbidelli A., 2005, *Natur*, 435, 466
- Hahn, J. M., Malhotra, R., 1999, *The Astronomical Journal* 117, 3041
- Hansen B. M. S., 2009, *ApJ*, 703, 1131
- Laskar J., 1997, *A&A*, 317, L75
- Laskar J., 2008, *Icar*, 196, 1
- Levison H. F., Duncan M. J., 1994, *Icar*, 108, 18
- Minton, D. A., Malhotra, R., 2009, *Nature* 457, 1109
- Morbidelli A., Levison H. F., Tsiganis K., Gomes R., 2005, *Natur*, 435, 462
- Morbidelli A., Tsiganis K., Crida A., Levison H. F., Gomes R., 2007, *AJ*, 134, 1790
- Morbidelli A., Brasser R., Tsiganis K., Gomes R., Levison H. F., 2009, *A&A*, 507, 1041
- Morbidelli A., Brasser R., Gomes R., Levison H. F., Tsiganis K., 2010, *AJ*, 140, 1391
- Nesvorný D., Vokrouhlický D., Morbidelli A., 2007, *AJ*, 133, 1962
- Nesvorný D., 2011, *ApJ*, 742, L22
- Nesvorný D., Morbidelli A., 2012, *AJ*, 144, 117
- Nesvorný D., Vokrouhlický D., Morbidelli A., 2013, *ApJ*, 768, 45
- Nobili A., Roxburgh I. W., 1986, *IAUS*, 114, 105
- O'Brien D. P., Morbidelli A., Levison H. F., 2006, *Icar*, 184, 39
- Raymond S. N., O'Brien D. P., Morbidelli A., Kaib N. A., 2009, *Icar*, 203, 644
- Pierens A., Nelson R. P., 2008, *A&A*, 482, 333
- Petit J.-M., Morbidelli A., Chambers J., 2001, *Icar*, 153, 338
- Thommes, E.W., Duncan, M. J., Levison, H. F., 1999, *Nature* 402, 635
- Tsiganis, K.; Gomes, R.; Morbidelli, A.; Levison, H. F., 2005, *Nature* 435, 459
- Saha P., Tremaine S., 1994, *AJ*, 108, 1962
- Walsh K. J., Morbidelli A., Raymond S. N., O'Brien D. P., Mandell, A. M., 2011, *Nature*, 475, 206
- Ward W. R., 1981, *Icar*, 47, 234